Algebraic equation of motion approach for solving the Anderson model

Hou-Min Du(杜厚旻) and Yu-Liang Liu(刘玉良)†

Department of Physics, Renmin University of China, Beijing 100872, *China*

(Received 18 April 2022; revised manuscript received 26 June 2022; accepted manuscript online 26 August 2022)

Based on the algebraic equation of motion (AEOM) approach, we have studied the single-impurity Anderson model by analytically solving the AEOM of the f-electron one-particle Green function in the Kondo limit. The related spectral function satisfies the sum rule and shows that there is a well-known three-peak structure at zero temperature. In the low energy limit, we obtain the analytical formula of the Kondo temperature that is the same as the exact solution in form except for a prefactor. We also show that the shape of the Kondo resonance is the Lorentzian form and the corresponding weight is proportional to the spin-flip correlation function.

Keywords: Anderson model, multiple-point correlation function, spin-flip correlation function

PACS: 75.20.Hr, 71.27.+a, 03.65.Fd **DOI:** 10.1088/1674-1056/ac8cdb

1. Introduction

The Anderson model[1] has been proposed to describe the local moments behavior of dilute magnetic alloys and is well understood.[2] With the development of semiconductor device technology, the local moments can be realized by quantum dots (QDs), and the tunable Kondo effect can be observed by adjusting the gate voltage.[3,4] On the other hand, the development of QD technology also provides a possible way to realize quantum computing.[5–7] Meanwhile, magnetic adatoms on the noble metal can also be controlled by the gate voltage, which serves as a quantum impurity system (QIS).[8–13]

In dilute magnetic alloys, the local moments can be thought of as independent from each other, which can be described by the single-impurity Anderson model (SIAM). As the concentration of magnetic atoms increases, however, the local moments are no longer independent from each other, as there is an indirect Ruderman–Kittel–Kasuya–Yosida (RKKY) interaction induced through the conduction band electrons.[14–16] In such a system, there are two energy scales, one is the Kondo temperature $T_{\rm K}$, below which the local moments tend to be screened by conduction band electrons, and the other is the RKKY interaction energy $T_{\rm RKKY}$, which can lead to a singlet between the local moments. The competition between these two energy scales may give rise to a quantum phase transition between the antiferromagnetic regime and the heavy-fermion regime, which is a function of $T_{\rm RKKY}/T_{\rm K}$.[17]

The two-impurity Kondo or Anderson model is considered to be the simplest model for investigating the above competition and is expected to shed light on the physics of heavy fermion systems. These models have been studied theoretically[18–30] and experimentally[10–13] over the past few decades. The most striking result is that at a certain ratio, $T_{\rm RKKY}/T_{\rm K}$, there is a quantum critical point (QCP) between the Kondo and the RKKY phases. Yet it is known that the QCP is sensitive to the particle–hole symmetry of the system, without which the system would transform into a crossover regime.[24]

Although the thermodynamic properties of the two-impurity Anderson model (TIAM) are well understood, the dynamical properties as a function of the distance between the impurities have not yet been comprehensively studied. Moreover, in most numerical studies, the RKKY interaction is treated as a direct interaction, however, the indirect RKKY interaction induced by conduction band electrons has not been clearly studied. Efficiently dealing with the strong on-site repulsive Coulomb interaction is a key point for understanding the electronic properties of strongly correlated systems. As a result, it is inappropriate to apply the usual perturbation theory to the TIAM.

In this paper, beyond the usual equation of motion (EOM) of Green function (GF) approaches,[31–37] we use the AEOM approach[38–40] to study the SIAM in the Kondo limit[41] and use it as a benchmark to test this approach. In contrast with the usual EOMs of a GF, which are usually written out in k-space, we write out the AEOMs in lattice space for the SIAM, and then we take the cut-off approximation for those higher-order multiple-point correlation functions in the AEOMs (see the appendix). There are two salient features in this approach: one is that the contributions coming from the on-site repulsive Coulomb interaction term can be effectively incorporated into the AEOMs, which is really represented by the related hierarchical multiple-point correlation functions; the other is that all the AEOMs together constitute a hierarchical structure which can be classified by the parameter N which labels the

†Corresponding author. E-mail: ylliu@ruc.edu.cn

© 2023 Chinese Physical Society and IOP Publishing Ltd

number of electrons residing in a length (sites) scale that take part in a time evolution of an electron from the initial to the final state. The multiple-point correlation functions in the same level N constitute some linear equations in which there may be a few multiple-point correlation functions belonging to the $N+1$ level. The physical meaning of the multiple-point correlation function in lattice space is very clear. It represents the time evolution of an electron from the site x_i at time t_1 to the site x_j at time t_2 meanwhile incorporating the effect of other electrons of number N around the initial site. It is expected that the multiple-point correlation functions belonging to the $N+1$ level have less effect in N level AEOMs so that we can take the cut-off approximation to them. In this way, we can obtain closed AEOMs and thus the f-electron one-particle GF.

As a consequence of applying the AEOM approach to the SIAM, we analytically calculate the f-electron one-particle GF and obtain the spectral function which has a well-known three-peak structure. The result shows that the total spectral weight of the f-electron one-particle GF is equal to unity. Meanwhile, in the low energy limit, we derive the explicit Kondo temperature formula from the pole which related to the Kondo resonance. In addition, it is remarkable that the shape of the Kondo resonance is the Lorentzian form[8,9] and the corresponding weight is proportional to the spin-flip correlation function. This result gives us an inspiration to calculate the excitation spectrum of the TIAM by searching for the related spin–spin correlation functions between the local moments. Calculation details are in the appendix.

2. Method

2.1. The formalism of the usual EOMs

In this section, we will briefly review the usual EOM approaches. Nagaoka first applied the EOM approach to the Kondo model,[31] and then based on this approach, the SIAM was extensively studied by improving his approach and obtained results[32–37] beyond the Hartree–Fock approximation by Anderson.[1] In the above approaches, the decoupling of the equations is usually to approximate the higher-order correlation functions, such as $\langle\langle c_{k\sigma}c_{q\bar{\sigma}}f^{\dagger}_{\bar{\sigma}}, f^{\dagger}_{\sigma}\rangle\rangle_{\omega} \simeq -\langle f^{\dagger}_{\bar{\sigma}}c_{q\bar{\sigma}}\rangle\langle\langle c_{k\sigma}, f^{\dagger}_{\sigma}\rangle\rangle$,[32] where $c^{\dagger}_{\sigma}$ and $f^{\dagger}_{\sigma}$ are respectively the creation operators for conduction and f electrons. In this way, all the EOMs are closed. However, the average values produced in the decoupling processes must be solved self-consistently by the fluctuation-dissipation theorem

$$\langle BA\rangle = \int_{-\infty}^{+\infty}\{-2\mathrm{Im}\langle\langle A,B\rangle\rangle_{\omega}\}\, f(\omega)\,\mathrm{d}\omega, \tag{1}$$

where $f(\omega)$ is the Fermi distribution function, which leads to the fact that the final f-electron one-particle GF is actually a very complicated integral equation, and further approximations must be taken to solve it. Usually, one solves the above integral equation in the limit $U\to\infty$, however, a realistic repulsive Coulomb interaction U is finite and is important to determine the spectral function.

In order to avoid the difficulties encountered by the above approaches, we recently proposed the AEOM approach to solve the SIAM. Due to the hierarchical nature of the AEOMs, we take the cut-off approximation to the higher-order multiple-point correlation functions at a high level AEOM to make all the AEOMs closed. From this, we have obtained a set of algebraic equations, and through algebraic calculations, we can obtain the final analytical f-electron one-particle GF. There are some static correlation functions in the AEOMs, however, the present approach only shows the influence of them on the weight of the spectral function and cannot determine the values of them.

2.2. The formalism of the AEOMs

The Hamiltonian of the SIAM in lattice space in which an impurity is fixed at site $\boldsymbol{x}_0$ is as follows:

$$\begin{aligned} H \;=\; & -t_0\sum_{ij\sigma}\gamma_{ij}\left(\hat{c}^{\dagger}_{i\sigma}\hat{c}_{j\sigma}+\hat{c}^{\dagger}_{j\sigma}\hat{c}_{i\sigma}\right)+V_0\sum_{\sigma}\left(\hat{f}^{\dagger}_{\sigma}\hat{c}_{0\sigma}+\hat{c}^{\dagger}_{0\sigma}\hat{f}_{\sigma}\right)\\ & +\sum_{\sigma}\varepsilon_f\hat{f}^{\dagger}_{\sigma}\hat{f}_{\sigma}+U\sum_{\sigma}\hat{n}_{f\bar{\sigma}}\hat{n}_{f\sigma}, \end{aligned} \tag{2}$$

where $\hat{c}^{\dagger}_{i\sigma}$ ($\hat{c}_{i\sigma}$) creates (annihilates) a conduction band electron with spin $\sigma=\uparrow,\downarrow$ at site $\boldsymbol{x}_i$, $\hat{n}_{f\sigma}=\hat{f}^{\dagger}_{\sigma}\hat{f}_{\sigma}$ is the number operator of the f-electron, t_0 is the hopping strength, V_0 is the s–f hybridization strength which is assumed to be a constant, ε_f is the f-electron energy level and U is the on-site repulsive Coulomb interaction strength. The hopping factor γ_{ij} is defined as

$$\gamma_{ij}=\begin{cases}1, & j=i\pm1,\\ 0, & j\neq i\pm1,\end{cases}$$

which denotes the summation over the sites $\boldsymbol{x}_i$, $\boldsymbol{x}_j$ only in the nearest neighbor. In this paper, the energy level of the impurity is set by $\varepsilon_f=-U/2$, and the energy of the system is measured from the Fermi level.

The f-electron one-particle GF in lattice space using the Heisenberg picture is defined as (choosing $\hbar=1$),

$$\begin{aligned} G_{\sigma}(t_1,t_2) \;=\; & -\mathrm{i}\theta(t_1-t_2)\left\langle\hat{f}_{\sigma}(t_1)\hat{f}^{\dagger}_{\sigma}(t_2)\right\rangle\\ & +\mathrm{i}\theta(t_2-t_1)\left\langle\hat{f}^{\dagger}_{\sigma}(t_2)\hat{f}_{\sigma}(t_1)\right\rangle, \end{aligned} \tag{3}$$

where the f-electron is fixed at site $\boldsymbol{x}_0=0$, $\langle\cdots\rangle$ denotes the exact ground state average. Applying the AEOM approach to the SIAM, we can write out the AEOM of the f-electron one-particle GF

$$\begin{aligned} \mathrm{i}\partial_{t_1}G_{\sigma}(t_1,t_2) \;=\; & \delta(t_1-t_2)+\varepsilon_f G_{\sigma}(t_1,t_2)\\ & +V_0\tilde{G}_{0\sigma}(t_1,t_2)+UF^{(n_{\bar{\sigma}})}_{\sigma}(t_1,t_2), \end{aligned} \tag{4}$$

where $\tilde{G}_{0\sigma}(t_1,t_2)=-\mathrm{i}\langle\hat{T}\hat{c}_{0\sigma}(t_1)\hat{f}^{\dagger}_{\sigma}(t_2)\rangle$ is the mixed GF, and $F^{(n_{\bar{\sigma}})}_{\sigma}(t_1,t_2)=-\mathrm{i}\langle\hat{T}\hat{n}_{f\bar{\sigma}}(t_1)\hat{f}_{\sigma}(t_1)\hat{f}^{\dagger}_{\sigma}(t_2)\rangle$ is the multiple-point

correlation function where $\hat{n}_{f\bar{\sigma}} = \hat{f}^{\dagger}_{\bar{\sigma}}\hat{f}_{\bar{\sigma}}$. The AEOM of the mixed GF can be written as

$$\mathrm{i}\partial_{t_1}\tilde{G}_{0\sigma}(t_1,t_2) = \sum_j h_{0j}\tilde{G}_{j\sigma}(t_1,t_2) + V_0 G_{\sigma}(t_1,t_2). \tag{5}$$

Its contribution to the f-electron one-particle GF is the effect of the hybridization between conduction band electrons and the f-electron. The multiple-point correlation function $F^{(n_{\bar{\sigma}})}_{\sigma}(t_1,t_2)$ is produced by the on-site repulsive Coulomb interaction and we can see that all the strong correlation effects of electrons originate completely from it. Meanwhile, it is precisely because of the existence of the on-site repulsive Coulomb interaction that the spin-flip scattering processes will happen. This multiple-point correlation function thus plays a key role in contributing the correlation effects to the f-electron one-particle GF.

The AEOM of the multiple-point correlation function $F^{(n_{\bar{\sigma}})}_{\sigma}(t_1,t_2)$ can be written as

$$\begin{aligned}\omega F^{(n_{\bar{\sigma}})}_{\sigma}(\omega) \;=\; & \langle \hat{n}_{f\bar{\sigma}} \rangle + \left(\varepsilon_f + U\right) F^{(n_{\bar{\sigma}})}_{\sigma}(\omega) \\ & + V_0 F^{(X^{(-)}_{\bar{\sigma}})}_{0\sigma}(\omega) + V_0 \tilde{F}^{(n_{\bar{\sigma}})}_{0\sigma}(\omega),\end{aligned} \tag{6}$$

where the definition of the new multiple-point correlation functions appearing in the above equation is given in Appendix B. We find that there appears the same multiple-point correlation function $F^{(n_{\bar{\sigma}})}_{\sigma}(\omega)$ in the above AEOM. Hence we will take the cut-off approximation for the new multiple-point correlation functions in Eq. (6). Before moving on, we must point out that before taking any approximation, equation (6) is rigorous and the Coulomb interaction U can be effectively incorporated in the AEOMs in the $N = 1$ level, which is qualitatively distinct from the usual perturbation theory that expands the GF in a power series of the U.[42]

Equations (4)–(6) are the key ones that we use to calculate the f-electron one-particle GF in the Kondo limit. Next, we write out the AEOMs of the new multiple-point correlation functions appearing in Eq. (6),

$$\begin{aligned}& \omega \tilde{F}^{(n_{\bar{\sigma}})}_{i\sigma}(\omega) \\ =\; & \sum_j h_{ij}\tilde{F}^{(n_{\bar{\sigma}})}_{j\sigma}(\omega) + V_0 \tilde{F}^{(X^{(-)}_{\bar{\sigma}})}_{0i\sigma}(\omega) + \delta_{i0} V_0 F^{(n_{\bar{\sigma}})}_{\sigma}(\omega),\end{aligned} \tag{7}$$

$$\begin{aligned}& \omega F^{(X^{(-)}_{\bar{\sigma}})}_{i\sigma}(\omega) \\ =\; & \left\langle \hat{X}^{(-)}_{i\bar{\sigma}} \right\rangle + \sum_j \left(h_{ij} - \delta_{ij}\varepsilon_f\right) F^{(X^{(+)}_{\bar{\sigma}})}_{j\sigma}(\omega) \\ & - V_0 F^{(Y^{(+)}_{\bar{\sigma}})}_{i0\sigma}(\omega) + \varepsilon_f F^{(X^{(-)}_{\bar{\sigma}})}_{i\sigma}(\omega) + V_0 \tilde{F}^{(X^{(-)}_{\bar{\sigma}})}_{i0\sigma}(\omega) \\ & + \frac{U}{2} F^{(X^{(-)}_{\bar{\sigma}})}_{i\sigma}(\omega) - \frac{U}{2} F^{(X^{(+)}_{\bar{\sigma}})}_{i\sigma}(\omega) + 2\delta_{i0} V_0 F^{(n_{\bar{\sigma}})}_{\sigma}(\omega),\end{aligned} \tag{8}$$

where more new multiple-point correlation functions emerge. With the same procedures, we can write out the AEOMs of these new multiple-point correlation functions in which there will appear more higher-order new correlation functions, and this set of AEOMs is not closed in the thermodynamic limit. In order to calculate the f-electron one-particle GF, we need to cut off this set of AEOMs in the Kondo limit. For large N level (see Appendix B), the related lattice sites of the multiple-point correlation functions are far away from $\boldsymbol{x}_0$, and the contributions of these functions to the f-electron one-particle GF are expected to be small so that we can safely take the cut-off approximation to them. In this paper, we take the cut-off approximation to the $N = 2$ level.

Figure 1 depicts the above discussion and gives the basic framework of the calculations. First, we keep the AEOMs of the multiple-point correlation function $F^{(X^{(-)}_{\bar{\sigma}})}_{i\sigma}(\omega)$ rigorous. Then, as lattice sites move away from $\boldsymbol{x}_0$, the contributions of the corresponding multiple-point correlation functions become increasingly small, and we can safely take the cut-off approximation to them. In contrast with the usual EOM of GF approaches, the current approach has a clearer physical picture and a more concise calculation framework.

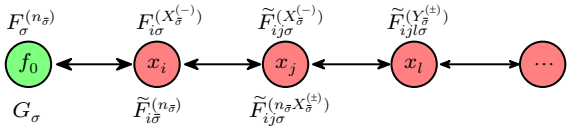


Fig. 1. A schematic of the multiple-point correlation functions in one spatial dimension. The red nodes represent conduction band electrons at lattice sites, and the green node represents the local f-electron fixed at $\boldsymbol{x}_0$. Above and/or below each node are their corresponding multiple-point correlation functions. The thickness of the arrows reflects the magnitude of the effect of multiple-point correlation functions on the f-electron one-particle GF.

The related multiple-point correlation function $F^{(X^{(-)}_{\bar{\sigma}})}_{0\sigma}(\omega)$ appearing in Eq. (6) plays a key role in calculating the f-electron one-particle GF, and makes significant contributions to the self-energy of the f-electron. In the Kondo limit, its analytical expression is given in Appendix C.

As for the AEOMs of the higher-order multiple-point correlation functions $\tilde{F}^{(n_{\sigma}X^{(\pm)}_{\bar{\sigma}})}_{ji\sigma}(\omega)$ which contain the spin-flip correlation functions (see Appendix C), we take the cut-off approximation to them that simply discards the terms different from the $\tilde{F}^{(n_{\sigma}X^{(\pm)}_{\bar{\sigma}})}_{ji\sigma}(\omega)$ in the $N = 2$ level. Meanwhile, we retain the spin-flip correlation functions rather than treating them as zero.[34] In order to save space, we only explicitly write out the approximated AEOMs in the low energy limit, so that we then have

$$\tilde{F}^{(n_{\sigma}X^{(\pm)}_{\bar{\sigma}})}_{ji\sigma}(\omega) \overset{\omega\to 0}{=} -\frac{1}{2}\frac{C_{ij}}{\varepsilon_f + U}, \tag{9}$$

where $C_{ij} = \langle [\hat{S}^{(+)}\hat{s}^{(-)}_{ji} + \hat{S}^{(-)}\hat{s}^{(+)}_{ji}] \rangle$ with $\hat{s}^{(+)}_{ji} = \hat{c}^{\dagger}_{j\uparrow}\hat{c}_{i\downarrow}$, $\hat{s}^{(-)}_{ji} = \hat{c}^{\dagger}_{j\downarrow}\hat{c}_{i\uparrow}$, $\hat{S}^{(+)} = \hat{f}^{\dagger}_{\downarrow}\hat{f}_{\uparrow}$, and $\hat{S}^{(-)} = \hat{f}^{\dagger}_{\uparrow}\hat{f}_{\downarrow}$, which represents the processes of spin-flip scattering. Actually, C_{ij} is a static correla-

tion function that we need to calculate self-consistently. However, the AEOM approach cannot determine the value of the static correlation function. In this paper, we treat it as a parameter.

3. Results

With the help of the analytical expression of the correlation function $F_{0\sigma}^{(X_{\bar{\sigma}}^{(-)})}(\omega)$ in Appendix C, we can obtain the following f-electron one-particle GF:

$$G_\sigma(\omega) = \frac{A}{\omega-\varepsilon_f-\Gamma_{00}^{(-)}(\omega)V_0^2}+\frac{B}{\omega-\varepsilon_f-U-\Gamma_{00}^{(-)}(\omega)V_0^2} +\frac{C}{\omega-[\varepsilon_f+\eta(\omega)]-\Delta(\omega)} \tag{10}$$

with

$$\begin{aligned} A &= 1-n_{f\bar{\sigma}}+\frac{Jn_{f\bar{\sigma}}}{2D(\omega)} \\ &\quad -\frac{1}{8}\frac{U^2C_{00}}{\varepsilon_f+U}\frac{J}{D(\omega)}\frac{1}{\Gamma_{00}^{(-)}(\omega)V_0^2-\eta(\omega)-\Delta(\omega)}, \\ B &= n_{f\bar{\sigma}}-\frac{Jn_{f\bar{\sigma}}}{2D(\omega)} \\ &\quad +\frac{1}{8}\frac{U^2C_{00}}{\varepsilon_f+U}\frac{J}{D(\omega)}\frac{1}{U+\Gamma_{00}^{(-)}(\omega)V_0^2-\eta(\omega)-\Delta(\omega)}, \\ C &= \frac{1}{8}\frac{U^2C_{00}}{\varepsilon_f+U}\frac{J}{D(\omega)}\frac{1}{\Gamma_{00}^{(-)}(\omega)V_0^2-\eta(\omega)-\Delta(\omega)} \\ &\quad -\frac{1}{8}\frac{U^2C_{00}}{\varepsilon_f+U}\frac{J}{D(\omega)}\frac{1}{U+\Gamma_{00}^{(-)}(\omega)V_0^2-\eta(\omega)-\Delta(\omega)}, \end{aligned}$$

where $n_{f\bar{\sigma}}=\langle\hat{n}_{f\bar{\sigma}}\rangle$ as a parameter, $\Gamma_{00}^{(\pm)}(\omega)=\frac{1}{N}\sum_k\frac{1}{\omega\pm\varepsilon_k}$, $\Delta(\omega)=\frac{V_0^2\Sigma_{00}^{(+)}(\omega)}{2}$, $\eta(\omega)=\frac{V_0^2\Sigma_{00}^{(-)}(\omega)}{2}$ with $\Sigma_{00}^{(\pm)}(\omega)=\Gamma_{00}^{(-)}(\omega)\pm\Gamma_{00}^{(+)}(\omega)$, and $D(\omega)=[\omega-\varepsilon_f-\frac{U}{2}+\frac{JU}{U+\Gamma_{00}^{(-)}(\omega)V_0^2}]$. Here $J=4V_0^2/U$ can be understood as the spin–spin coupling strength which is naturally generated from the decoupling processes.

From Eq. (10), we find that if C_{00} equals zero, the density of states (DOS) of the f-electron one-particle GF will have only two resonances at $\pm U/2$, which corresponds to the known results from the Hartree–Fock approximation. Considering the effect of spin-flip scattering, we notice that there appears a third resonance which is strongly affected by the spin-flip correlation function.

Now we write the third pole explicitly, which reads

$$\omega=\varepsilon_f+\frac{V_0^2\rho(0)}{2}\int_{-D}^{D}\mathrm{d}\varepsilon\theta(-\varepsilon)\left(\frac{1}{\omega-\varepsilon}-\frac{1}{\omega+\varepsilon}\right)+\Delta(\omega), \tag{11}$$

where D is the half-bandwidth of the conduction band and $\rho(0)$ is the DOS of conduction band electrons which has been assumed to be a constant for a broad conduction band. By replacing ω with $\omega+\mathrm{i}0^+$ in $\Delta(\omega)$, we have the imaginary part of the self-energy, that is

$$\mathrm{Im}\Delta(\omega+\mathrm{i}0^+)=-\frac{\pi V_0^2\rho(0)}{2}. \tag{12}$$

For the real part of $\Delta(\omega+\mathrm{i}0^+)$, we have neglected in the particle–hole symmetric case. As the value of V_0 is relatively small, the shape of the Kondo resonance is the Lorentzian form.

In the low energy limit, or zero temperature, we integrate out the conduction band electrons' energy and obtain the following formula:

$$\omega=\varepsilon_f-\rho(0)V_0^2\ln\left|\frac{\omega}{D}\right|. \tag{13}$$

This dispersion is very similar to the renormalized level of the f-electron which was obtained by using the scaling theory[43] and the EOM approach,[32] respectively. And the Kondo temperature can be defined as

$$T_\mathrm{K}=D\exp\left[-\frac{U\pi}{2\Delta}\right], \tag{14}$$

where $\Delta=\pi\rho(0)V_0^2$. The above result is the same as the exact one except for a prefactor.[44]

It is worth noting the relationship between the conduction band electron and the f-electron one-particle GFs. In the former, the logarithmic terms appear in the imaginary part of the retarded self-energy contributed by the latter which plays the role of the scattering t-matrix, and thus the Kondo effect appears. While for the latter, the Kondo effect shows that there is a renormalized f-electron level corresponding to the low-lying excitation of the system, which is strongly affected by the spin-flip scattering. This renormalized level characterizes the nonanalytic energy scale T_K of the system, below which the ground state is a local Fermi liquid where the quasiparticles are the so-called Kondo cloud.

According to the expression for the f-electron one-particle GF, we find that the spectral function, $A_{f\sigma}(\omega)=-2\mathrm{Im}G_\sigma(\omega+\mathrm{i}0^+)$, satisfies the sum rule, that is

$$\frac{1}{2\pi}\int_{-\infty}^{\infty}\mathrm{d}\omega A_{f\sigma}(\omega)=1, \tag{15}$$

which is independent of the approximations taken in solving the AEOMs of the multiple-point correlation functions. In the low energy limit, the coefficients A, B, and C in Eq. (10) are reduced to

$$A\overset{\omega\to0}{=}\frac{3}{4}+\frac{C_{00}}{2},\quad B\overset{\omega\to0}{=}\frac{1}{4}+\frac{C_{00}}{2},\quad C\overset{\omega\to0}{=}-C_{00}, \tag{16}$$

where we have set $n_{f\bar{\sigma}}=1/2$. Following the above results, we can see the influence of the spin-flip correlation function on the Kondo resonance more clearly.

Figure 2 clearly shows the resulting spectral function for various values of C_{00}. The DOS shows that there is a well-known three-peak structure, the charge-fluctuation peaks at $\pm U/2$ and the Kondo resonance peak near the Fermi level. The shape of the Kondo resonance is a Lorentzian lineshape which is consistent with the experimentally observed differential conductance spectrum.[8,9] With the increasing of C_{00}, which is the spin-flip correlation function representing the spin-fluctuation between conduction band electrons and the f-electron, the spectral weight of the Kondo resonance is continuously increasing. However, the parameter C_{00} only describes the spin-flip on the single site of the f-electron. In fact, in the low energy limit, the spin degree of freedom of the f-electron has been quenched by all the surrounding electrons, and the spin-flip correlation function is largely dependent on the influence of the local environment.[9] Meanwhile, we find that the lower and upper Hubbard bands are not actually symmetrical even though the C_{00} equals zero. The stronger the spin-flip strength is, the more spectral weights are transferred from the upper Hubbard band to the lower Hubbard band.

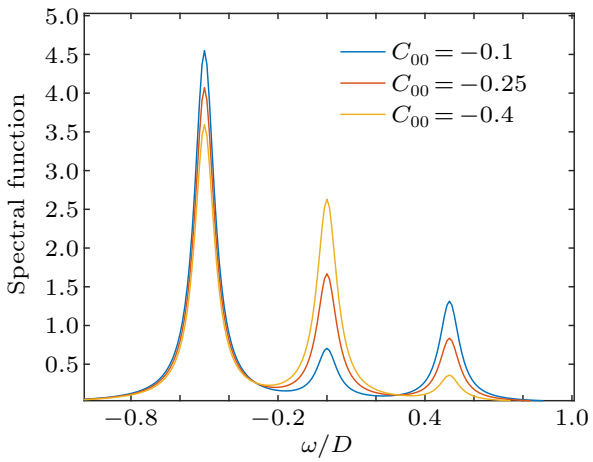


Fig. 2. Spectral function for the f-electron in $T=0$ K. The selective values of the corresponding parameters are $V_0=0.25$, $D=1$, $U=1$, and $\rho(0)=1/2D$. The Kondo temperature is close to 0.

4. Summary and perspective

In summary, we propose a new formalism that is essentially distinct from the usual EOM of GF approaches, that is the AEOM approach in which the AEOMs are written out in lattice space. We apply it to the SIAM in the Kondo limit. Under the cut-off approximation, we analytically calculate the one-particle GF of the f-electron and obtain the corresponding spectral function, which has the well-known three-peak structure where the shape of the Kondo resonance is the Lorentzian form. In the low energy limit, we derive the Kondo temperature that depends exponentially on the strength of the interaction parameter U. Finally, we demonstrate that the spectral weight of the Kondo resonance is proportional to the spin-flip correlation function. The present results give us an inspiration to calculate the excitation spectrum of the TIAM by searching for the related spin–spin correlation functions between the local moments.

Appendix A: The basic commutation relations

In order to write out the AEOMs of the f-electron one-particle GF $G_\sigma(t_1,t_2)=-\mathrm{i}\langle\hat{T}\hat{f}(t_1)\hat{f}^\dagger(t_2)\rangle$ and related multiple-point correlation functions, we need to calculate the following commutation relations (choosing $\hbar=1$):

$$\left[\hat{n}_{f\bar{\sigma}},\hat{H}\right]=V_0\hat{X}_{0\bar{\sigma}}, \tag{A1}$$

$$\left[\hat{c}_{i\sigma},\hat{H}\right]=\sum_j h_{ij}\hat{c}_{j\sigma}+\delta_{i0}V_0\hat{f}_\sigma, \tag{A2}$$

$$\left[\hat{f}_\sigma,\hat{H}\right]=\varepsilon_f\hat{f}_\sigma+V_0\hat{c}_{0\sigma}+U\hat{n}_{f\sigma}\hat{f}_\sigma, \tag{A3}$$

$$\left[\hat{Y}^{(\pm)}_{ij\bar{\sigma}},\hat{H}\right]=\sum_m h_{im}\hat{Y}^{(\mp)}_{mj\bar{\sigma}}-\sum_m h_{jm}\hat{Y}^{(\mp)}_{im\bar{\sigma}} \mp\delta_{i0}V_0\hat{X}^{(\mp)}_{j\bar{\sigma}}-\delta_{j0}V_0\hat{X}^{(\mp)}_{i\bar{\sigma}}, \tag{A4}$$

$$\left[\hat{X}^{(+)}_{i\bar{\sigma}},\hat{H}\right]=\sum_j(h_{ij}-\delta_{ij})\hat{X}^{(-)}_{j\bar{\sigma}}-U\hat{n}_{f\sigma}\hat{X}^{(-)}_{i\bar{\sigma}} -V_0\hat{Y}^{(-)}_{i0\bar{\sigma}}, \tag{A5}$$

$$\left[\hat{X}^{(-)}_{i\bar{\sigma}},\hat{H}\right]=\sum_j(h_{ij}-\delta_{ij})\hat{X}^{(+)}_{j\bar{\sigma}}-U\hat{n}_{f\sigma}\hat{X}^{(+)}_{i\bar{\sigma}} +2\delta_{i0}V_0\hat{n}_{f\bar{\sigma}}-V_0\hat{Y}^{(+)}_{i0\bar{\sigma}}, \tag{A6}$$

where $h_{ij}=-t_0(\gamma_{ij}+\gamma_{ji})$, and the operators $\hat{X}^{(\pm)}_{i\sigma}$ and $\hat{Y}^{(\pm)}_{ij\sigma}$ are defined as $\hat{X}^{(\pm)}_{i\sigma}=\hat{f}^\dagger_\sigma\hat{c}_{i\sigma}\pm\hat{c}^\dagger_{i\sigma}\hat{f}_\sigma$ and $\hat{Y}^{(\pm)}_{ij\sigma}=\hat{c}^\dagger_{j\sigma}\hat{c}_{i\sigma}\pm\hat{c}^\dagger_{i\sigma}\hat{c}_{j\sigma}$, respectively. These commutation relations are the elementary ingredients in writing out the AEOMs of the related multiple-point correlation functions via Heisenberg EOMs.

Appendix B: Definition of multiple-point correlation functions

In order to tersely represent the correlation functions appearing in the hierarchical series of AEOMs, we introduce the multiple-point correlation functions

$$F^{(\{A\})}_{\{\alpha\}mq}(t_1,t_2)=-\mathrm{i}\left\langle\hat{T}\prod_{k=1}^{N}\left[\hat{A}_\alpha(t)\right]^k\hat{f}_{m\sigma}(t_1)\hat{f}^\dagger_{q\sigma}(t_2)\right\rangle, \tag{B1}$$

$$\tilde{F}^{(\{A\})}_{\{\alpha\}mq}(t_1,t_2)=-\mathrm{i}\left\langle\hat{T}\prod_{k=1}^{N}\left[\hat{A}_\alpha(t)\right]^k\hat{c}_{m\sigma}(t_1)\hat{f}^\dagger_{q\sigma}(t_2)\right\rangle, \tag{B2}$$

where $\hat{A}_\alpha=\{\hat{c}_{i\sigma},\hat{f}_\sigma,\hat{n}_{f\bar{\sigma}},\hat{X}^{(\pm)}_{i\bar{\sigma}},\hat{Y}^{(\pm)}_{ij\bar{\sigma}}\}$, α is a set of the lattice and spin index of each operator and N is the number of operators appearing in correlation functions, which represents the level of the corresponding correlation functions in all the AEOMs.

In contrast with the traditional correlation functions defined in k-space, the present multiple-point correlation functions give a clearer physical picture of the correlated electrons, and represent the evolution processes of an electron from the

initial lattice site, incorporating the influence of a definite distribution of other electrons around this electron, to the final lattice site. And the related multiple-point correlation functions which are derived from the on-site repulsive Coulomb interaction can be effectively incorporated in the AEOMs.

Appendix C: Solutions of the high-order multiple-point correlation functions

Based on the basic commutation relations in Eqs. (A1)–(A6), we can write out the following AEOMs after taking the Fourier transformation of time:

$$\begin{aligned}\omega\tilde{F}^{(X^{(-)}_{\tilde{\sigma}})}_{ji\sigma}(\omega) &= \left(h_{jm}-\delta_{jm}\varepsilon_f\right)\tilde{F}^{(X^{(+)}_{\tilde{\sigma}})}_{mi\sigma}(\omega)-U\tilde{F}^{(n_\sigma X^{(+)}_{\tilde{\sigma}})}_{ji\sigma}(\omega)\\ &\quad -V_0\tilde{F}^{(Y^{(+)}_{\tilde{\sigma}})}_{j0i\sigma}(\omega)+h_{im}\tilde{F}^{(X^{(-)}_{\tilde{\sigma}})}_{jm\sigma}(\omega)\\ &\quad +\delta_{i0}V_0F^{(X^{(-)}_{\sigma})}_{j\sigma}(\omega)+2\delta_{j0}V_0\tilde{F}^{(n_{\tilde{\sigma}})}_{i\sigma}(\omega), \quad \text{(C1)}\\ \omega\tilde{F}^{(X^{(+)}_{\tilde{\sigma}})}_{ji\sigma}(\omega) &= \left(h_{jm}-\delta_{jm}\varepsilon_f\right)\tilde{F}^{(X^{(-)}_{\tilde{\sigma}})}_{mi\sigma}(\omega)-U\tilde{F}^{(n_\sigma X^{(-)}_{\tilde{\sigma}})}_{ji\sigma}(\omega)\\ &\quad -V_0\tilde{F}^{(Y^{(-)}_{\tilde{\sigma}})}_{j0i\sigma}(\omega)+h_{im}\tilde{F}^{(X^{(+)}_{\tilde{\sigma}})}_{jm\sigma}(\omega)\\ &\quad +\delta_{i0}V_0F^{(X^{(+)}_{\sigma})}_{j\sigma}(\omega), \quad \text{(C2)}\\ \omega\tilde{F}^{(Y^{(-)}_{\tilde{\sigma}})}_{lji\sigma}(\omega) &= h_{lm}\tilde{F}^{(Y^{(+)}_{\tilde{\sigma}})}_{mji\sigma}(\omega)-h_{jm}\tilde{F}^{(Y^{(+)}_{\tilde{\sigma}})}_{lmi\sigma}(\omega)\\ &\quad +\delta_{l0}V_0\tilde{F}^{(X^{(+)}_{\tilde{\sigma}})}_{ji\sigma}(\omega)-\delta_{j0}V_0\tilde{F}^{(X^{(+)}_{\tilde{\sigma}})}_{li\sigma}(\omega)\\ &\quad +h_{im}\tilde{F}^{(Y^{(-)}_{\tilde{\sigma}})}_{ljm\sigma}(\omega)+\delta_{i0}V_0F^{(Y^{(-)}_{\tilde{\sigma}})}_{lj\sigma}(\omega), \quad \text{(C3)}\\ \omega\tilde{F}^{(Y^{(+)}_{\tilde{\sigma}})}_{lji\sigma}(\omega) &= h_{lm}\tilde{F}^{(Y^{(-)}_{\tilde{\sigma}})}_{mji\sigma}(\omega)-h_{jm}\tilde{F}^{(Y^{(-)}_{\tilde{\sigma}})}_{lmi\sigma}(\omega)\\ &\quad -\delta_{l0}V_0\tilde{F}^{(X^{(-)}_{\tilde{\sigma}})}_{ji\sigma}(\omega)-\delta_{j0}V_0\tilde{F}^{(X^{(-)}_{\tilde{\sigma}})}_{li\sigma}(\omega)\\ &\quad +h_{im}\tilde{F}^{(Y^{(+)}_{\tilde{\sigma}})}_{ljm\sigma}(\omega)+\delta_{i0}V_0F^{(Y^{(+)}_{\tilde{\sigma}})}_{lj\sigma}(\omega), \quad \text{(C4)}\end{aligned}$$

where we have used the Einstein summation convention. So far we have written out all the AEOMs of multiple-point correlation functions that we needed in the $N=1$ level. In order to decouple the above AEOMs, we need to take the cut-off approximation in the Kondo limit, that is $U \gg V_0$, and the impurity energy level is well below the Fermi level.

After taking the cut-off approximation in which we discard the lower-order terms to ensure Eqs. (C1)–(C4) are closed so as to decouple them, we have

$$\begin{aligned}\omega\tilde{F}^{(X^{(-)}_{\tilde{\sigma}})}_{ji\sigma}(\omega) &= -\varepsilon_f\tilde{F}^{(X^{(+)}_{\tilde{\sigma}})}_{ji\sigma}(\omega)-U\tilde{F}^{(n_\sigma X^{(+)}_{\tilde{\sigma}})}_{ji\sigma}(\omega)\\ &\quad -V_0\tilde{F}^{(Y^{(+)}_{\tilde{\sigma}})}_{j0i\sigma}(\omega), \quad \text{(C5)}\\ \omega\tilde{F}^{(X^{(+)}_{\tilde{\sigma}})}_{ji\sigma}(\omega) &= -\varepsilon_f\tilde{F}^{(X^{(-)}_{\tilde{\sigma}})}_{ji\sigma}(\omega)-U\tilde{F}^{(n_\sigma X^{(-)}_{\tilde{\sigma}})}_{ji\sigma}(\omega)\\ &\quad -V_0\tilde{F}^{(Y^{(-)}_{\tilde{\sigma}})}_{j0i\sigma}(\omega), \quad \text{(C6)}\\ \omega\tilde{F}^{(Y^{(-)}_{\tilde{\sigma}})}_{lji\sigma}(\omega)+h_{jm}\tilde{F}^{(Y^{(+)}_{\tilde{\sigma}})}_{lmi\sigma}(\omega)-h_{jm}\tilde{F}^{(Y^{(+)}_{\tilde{\sigma}})}_{mji\sigma}(\omega)&\\ &= -\delta_{j0}V_0\tilde{F}^{(X^{(+)}_{\tilde{\sigma}})}_{li\sigma}(\omega), \quad \text{(C7)}\\ \omega\tilde{F}^{(Y^{(+)}_{\tilde{\sigma}})}_{lji\sigma}(\omega)+h_{jm}\tilde{F}^{(Y^{(-)}_{\tilde{\sigma}})}_{lmi\sigma}(\omega)-h_{jm}\tilde{F}^{(Y^{(-)}_{\tilde{\sigma}})}_{mji\sigma}(\omega)&\\ &= -\delta_{j0}V_0\tilde{F}^{(X^{(-)}_{\tilde{\sigma}})}_{li\sigma}(\omega), \quad \text{(C8)}\end{aligned}$$

where $\varepsilon_f = -U/2$. In the above approximations, we neglect the terms coupling with V_0 such as $V_0F^{(X^{(\pm)}_{\tilde{\sigma}})}_{j\sigma}(\omega)$, $V_0\tilde{F}^{(X^{(\pm)}_{\tilde{\sigma}})}_{ji\sigma}(\omega)$, and $V_0F^{(Y^{(\pm)}_{\tilde{\sigma}})}_{lj\sigma}(\omega)$, because these terms make relatively small contributions to the AEOMs in the Kondo limit. In this limit, one can take a second-order perturbation expansion with respect to V_0, which is equivalent to the Schrieffer–Wolff transformation,[41] and thus the SIAM transforms into the Kondo model which gives rise to the Kondo effect. In addition, we also neglect the terms coupling with the hopping strength such as $h_{jm}\tilde{F}^{(X^{(\pm)}_{\tilde{\sigma}})}_{mi\sigma}(\omega)$, $h_{im}\tilde{F}^{(X^{(\pm)}_{\tilde{\sigma}})}_{jm\sigma}(\omega)$, and $h_{im}\tilde{F}^{(Y^{(\pm)}_{\tilde{\sigma}})}_{ljm\sigma}(\omega)$, because these terms make small contributions to the AEOMs near the Fermi level. Actually, the cut-off energy D of the conduction band is of the same order as the Coulomb interaction U, and the present cut-off approximation is only valid near the Fermi level.

Then applying the Fourier transformation, that is $\tilde{F}^{(Y^{(\pm)}_{\tilde{\sigma}})}_{lji\sigma}(\omega)=\frac{1}{\sqrt{N}}\sum_k\tilde{F}^{(Y^{(\pm)}_{\tilde{\sigma}})}_{li\sigma}(\omega,k)\,\mathrm{e}^{\mathrm{i}k\cdot\boldsymbol{x}_j}$, to Eqs. (C7) and (C8) and making some simplifications, in which we neglect the particle excitation, we have

$$\begin{aligned}&\tilde{F}^{(Y^{(\pm)}_{\tilde{\sigma}})}_{lji\sigma}(\omega)\\ &= \frac{V_0\Sigma^{(-)}_{j0}(\omega)}{2}\tilde{F}^{(X^{(\pm)}_{\tilde{\sigma}})}_{li\sigma}(\omega)-\frac{V_0\Sigma^{(+)}_{j0}(\omega)}{2}\tilde{F}^{(X^{(\mp)}_{\tilde{\sigma}})}_{li\sigma}(\omega), \quad \text{(C9)}\end{aligned}$$

where $\Sigma^{(\pm)}_{j0}(\omega)=[\Gamma^{(-)}_{j0}(\omega)\pm\Gamma^{(+)}_{j0}(\omega)]\theta(-\varepsilon)$ with $\Gamma^{(\pm)}_{j0}=\frac{1}{N}\sum_k\frac{\mathrm{e}^{\mathrm{i}k\cdot(\boldsymbol{x}_j-\boldsymbol{x}_0)}}{\omega\pm\varepsilon_k}$.

Next we write out the following AEOMs of $\tilde{F}^{(n_\sigma X^{(\pm)}_{\tilde{\sigma}})}_{ji\sigma}(\omega)$ that belong to the $N=2$ level in Eqs. (C5) and (C6):

$$\begin{aligned}&\omega\tilde{F}^{(n_\sigma X^{(-)}_{\tilde{\sigma}})}_{ji\sigma}(\omega)\\ &= -\left\langle\hat{X}^{(-)}_{j\tilde{\sigma}}\hat{f}^{\dagger}_{\sigma}\hat{c}_{i\sigma}\right\rangle-U\tilde{F}^{(n_\sigma X^{(+)}_{\tilde{\sigma}})}_{ji\sigma}(\omega)+V_0\tilde{F}^{(X^{(-)}_{\sigma}X^{(-)}_{\tilde{\sigma}})}_{0ji\sigma}(\omega)\\ &\quad +\left(h_{jm}-\delta_{jm}\varepsilon_f\right)\tilde{F}^{(n_\sigma X^{(+)}_{\tilde{\sigma}})}_{mi\sigma}(\omega)-V_0\tilde{F}^{(n_\sigma Y^{(+)}_{\tilde{\sigma}})}_{j0i\sigma}(\omega)\\ &\quad +h_{im}\tilde{F}^{(n_\sigma X^{(-)}_{\tilde{\sigma}})}_{jm\sigma}(\omega)+2\delta_{j0}V_0\tilde{F}^{(n_\sigma n_{\bar{\sigma}})}_{i\sigma}(\omega), \quad \text{(C10)}\\ &\omega\tilde{F}^{(n_\sigma X^{(+)}_{\tilde{\sigma}})}_{ji\sigma}(\omega)\\ &= -\left\langle\hat{X}^{(+)}_{j\tilde{\sigma}}\hat{f}^{\dagger}_{\sigma}\hat{c}_{i\sigma}\right\rangle-U\tilde{F}^{(n_\sigma X^{(-)}_{\tilde{\sigma}})}_{ji\sigma}(\omega)+V_0\tilde{F}^{(X^{(-)}_{\sigma}X^{(+)}_{\tilde{\sigma}})}_{0ji\sigma}(\omega)\\ &\quad +\left(h_{jm}-\delta_{jm}\varepsilon_f\right)\tilde{F}^{(n_\sigma X^{(-)}_{\tilde{\sigma}})}_{mi\sigma}(\omega)-V_0\tilde{F}^{(n_\sigma Y^{(-)}_{\tilde{\sigma}})}_{j0i\sigma}(\omega)\\ &\quad +h_{im}\tilde{F}^{(n_\sigma X^{(+)}_{\tilde{\sigma}})}_{jm\sigma}(\omega). \quad \text{(C11)}\end{aligned}$$

For simplicity,we take the cut-off approximation that discards those multiple-point correlation functions in the $N=2$ level except for $\tilde{F}_{ji\sigma}^{(n_\sigma X_{\bar{\sigma}}^{(\pm)})}(\omega)$. In the low energy limit, we have

$$\tilde{F}_{ji\sigma}^{(n_\sigma X_{\bar{\sigma}}^{(\pm)})}(\omega) \overset{\omega\to 0}{=} \mp\frac{1}{2}\frac{\left\langle\left[\hat{S}^{(+)}\hat{s}_{ij}^{(-)}+\hat{S}^{(-)}\hat{s}_{ij}^{(+)}\right]\right\rangle}{\varepsilon_f+U}, \tag{C12}$$

where $\hat{s}_{ji}^{(+)}=\hat{c}_{j\uparrow}^{\dagger}\hat{c}_{i\downarrow}$, $\hat{s}_{ji}^{(-)}=\hat{c}_{j\downarrow}^{\dagger}\hat{c}_{i\uparrow}$, $\hat{S}^{(+)}=\hat{f}_{\downarrow}^{\dagger}\hat{f}_{\uparrow}$, $\hat{S}^{(-)}=\hat{f}_{\uparrow}^{\dagger}\hat{f}_{\downarrow}$ and we have averaged over the spin-flip processes.

Here, we do not further write out the other AEOMs of the multiple-point correlation functions belonging to the $N=2$ level, and we simply discard those multiple-point correlation functions belonging to the $N\geq 2$ level, because we find that the basic behavior of the spectral function does not change with the higher-level AEOMs entering. Next, we substitute the approximated multiple-point correlation functions $\tilde{F}_{ji\sigma}^{(n_\sigma X_{\bar{\sigma}}^{(\pm)})}(\omega)$ and $\tilde{F}_{j0i\sigma}^{(Y_{\bar{\sigma}}^{(\pm)})}(\omega)$ into Eqs. (C5) and (C6). Finally we obtain the self-energy part of the Kondo resonance

$$\tilde{F}_{ji\sigma}^{(X_{\bar{\sigma}}^{(-)})}(\omega)=\frac{1}{2}\frac{U}{\varepsilon_f+U}\frac{\left\langle\left[\hat{S}^{(+)}\hat{s}_{ij}^{(-)}+\hat{S}^{(-)}\hat{s}_{ij}^{(+)}\right]\right\rangle}{\omega-\left[\varepsilon_f+\eta(\omega)\right]-\Delta(\omega)}, \tag{C13}$$

where $\eta(\omega)=\frac{V_0^2\Sigma_{00}^{(-)}(\omega)}{2}$ and $\Delta(\omega)=\frac{V_0^2\Sigma_{00}^{(+)}(\omega)}{2}$.

Substituting the above solution in the AEOM of $F_{i\sigma}^{(X_{\bar{\sigma}}^{(-)})}(\omega)$ and discarding the function $F_{i0\sigma}^{(Y_{\bar{\sigma}}^{(+)})}(\omega)$, we have the following expression:

$$\begin{aligned}
&F_{0\sigma}^{(X_{\bar{\sigma}}^{(-)})}(\omega)\\
&=-\frac{1}{D(\omega)}\frac{2V_0 n_{f\bar{\sigma}}}{\varepsilon_f+U+\Gamma_{00}^{(-)}(\omega)V_0^2}\\
&\quad+\frac{1}{2}\frac{U}{\varepsilon_f+U}\frac{V_0}{D(\omega)}\frac{\left\langle\left[\hat{S}^{(+)}\hat{s}_{ij}^{(-)}+\hat{S}^{(-)}\hat{s}_{ij}^{(+)}\right]\right\rangle}{\omega-\Delta(\omega)-\left[\varepsilon_f+\eta(\omega)\right]},
\end{aligned} \tag{C14}$$

where $n_{f\bar{\sigma}}=\langle\hat{n}_{f\bar{\sigma}}\rangle$ as a parameter and $D(\omega)=[\omega-\varepsilon_f-\frac{U}{2}+\frac{JU}{U+\Gamma_{00}^{(-)}(\omega)V_0^2}]$.

Acknowledgment

Project supported by the National Natural Science Foundation of China (Grant No. 11974420).

References

[1] Anderson P W 1961 *Phys. Rev.* **124** 41
[2] Hewson A C 1997 *The Kondo Problem to Heavy Fermions* (Cambridge University Press)
[3] Goldhaber-Gordon D, Shtrikman H, Mahalu D, Abusch-Magder D, Meirav U and Kastner M 1998 *Nature* **391** 156
[4] Cronenwett S M, Oosterkamp T H and Kouwenhoven L P 1998 *Science* **281** 540
[5] Loss D and DiVincenzo D P 1998 *Phys. Rev. A* **57** 120
[6] Burkard G, Loss D and DiVincenzo D P 1999 *Phys. Rev. B* **59** 2070
[7] Trauzettel B, Bulaev D V, Loss D and Burkard G 2007 *Nat. Phys.* **3** 192
[8] Madhavan V, Chen W, Jamneala T, Crommie M and Wingreen N 1998 *Science* **280** 567
[9] Heinrich A J, Gupta J A, Lutz C P and Eigler D M 2004 *Science* **306** 466
[10] Bork J, Zhang Y h, Diekhöner L, Borda L, Simon P, Kroha J, Wahl P and Kern K 2011 *Nat. Phys.* **7** 901
[11] Prüser H, Dargel P E, Bouhassoune M, Ulbrich R G, Pruschke T, Lounis S and Wenderoth M 2014 *Nat. Commun.* **5** 5417
[12] Spinelli A, Gerrits M, Toskovic R, Bryant B, Ternes M and Otte A 2015 *Nat. Commun.* **6** 10046
[13] Chen W, Yan Y, Ren M, Zhang T and Feng D 2022 *Sci. China Phys. Mech.* **65** 246811
[14] Ruderman M A and Kittel C 1954 *Phys. Rev.* **96** 99
[15] Kasuya T 1956 *Prog. Theor. Phys.* **16** 45
[16] Yosida K 1957 *Phys. Rev.* **106** 893
[17] Doniach S 1977 *Physica B+C* **91** 231
[18] Jayaprakash C, Krishna-murthy H R and Wilkins J W 1981 *Phys. Rev. Lett.* **47** 737
[19] Jones B A and Varma C M 1987 *Phys. Rev. Lett.* **58** 843
[20] Jones B A, Varma C M and Wilkins J W 1988 *Phys. Rev. Lett.* **61** 125
[21] Sakai O, Shimizu Y and Kasuya T 1990 *Solid State Commun.* **75** 81
[22] Fye R M 1994 *Phys. Rev. Lett.* **72** 916
[23] Affleck I, Ludwig A W W and Jones B A 1995 *Phys. Rev. B* **52** 9528
[24] Silva J, Lima W, Oliveira W, Mello J, Oliveira L N D and Wilkins J 1996 *Phys. Rev. Lett.* **76** 275
[25] Zhu L and Zhu J X 2011 *Phys. Rev. B* **83** 195103
[26] He R Q, Dai J and Lu Z Y 2015 *Phys. Rev. B* **91** 155140
[27] Jabben T, Grewe N and Schmitt S 2012 *Phys. Rev. B* **85** 045133
[28] Lechtenberg B, Eickhoff F and Anders F B 2017 *Phys. Rev. B* **96** 041109
[29] Eickhoff F, Lechtenberg B and Anders F B 2018 *Phys. Rev. B* **98** 115103
[30] Nejati A, Ballmann K and Kroha J 2017 *Phys. Rev. Lett.* **118** 117204
[31] Nagaoka Y 1965 *Phys. Rev.* **138** A1112
[32] Lacroix C 1981 *J. Phys. F: Metal Phys.* **11** 2389
[33] Lacroix C 1982 *J. Appl. Phys.* **53** 2131
[34] Luo H G, Ying J J and Wang S J 1999 *Phys. Rev. B* **59** 9710
[35] Kang K and Min B I 1995 *Phys. Rev. B* **52** 10689
[36] Fan P, Yang K, Ma K H and Tong N H 2018 *Phys. Rev. B* **97** 165140
[37] Ming-Lun C and Shun-Jin W 2007 *Chin. Phys. B* **16** 2096
[38] Liu Y L 2018 *Int. J. Mod. Phys. B* **32** 1850258
[39] Liu Y L 2019 *Int. J. Mod. Phys. B* **33** 1950355
[40] Liu Y L 2021 *Int. J. Mod. Phys. B* **35** 2150064
[41] Schrieffer J R and Wolff P A 1966 *Phys. Rev.* **149** 491
[42] Yamada K 1975 *Prog. Theor. Phys.* **53** 970
[43] Haldane F D M 1978 *Phys. Rev. Lett.* **40** 416
[44] Wiegmann P B 1981 *J. Phys. C: Solid State Phys.* **14** 1463